Black Phosphorus Hot Paper

DOI: 10.1002/ange.201409400

Black Phosphorus Quantum Dots**

*Xiao Zhang, Haiming Xie, Zhengdong Liu, Chaoliang Tan, Zhimin Luo, Hai Li, Jiadan Lin, Liqun Sun, Wei Chen, Zhichuan Xu, Linghai Xie, Wei Huang, and Hua Zhang**

Abstract: *As a unique two-dimensional nanomaterial, layered black phosphorus (BP) nanosheets have shown promising applications in electronics. Although mechanical exfoliation was successfully used to prepare BP nanosheets, it is still a challenge to produce novel BP nanostructures in high yield. A facile top-down approach for preparation of black phosphorus quantum dots (BPQDs) in solution is presented. The obtained BPQDs have a lateral size of 4.9 ± 1.6 nm and thickness of 1.9 ± 0.9 nm (ca. 4 ± 2 layers). As a proof-of-concept application, by using BPQDs mixed with polyvinylpyrrolidone as the active layer, a flexible memory device was successfully fabricated that exhibits a nonvolatile rewritable memory effect with a high ON/OFF current ratio and good stability.*

Two-dimensional (2D) layered materials, such as graphene and transition-metal dichalcogenides (TMDs), have emerged as a class of promising nanomaterials in both fundament studies and potential applications owing to their intriguing properties.[1] Besides the 2D layered structure, ultra-small quantum dot (QD), as another form of nanomaterials, exhibits unique electronic and optical properties owing to the quantum confinement and edge effects.[2] For example, graphene and MoS_2 QDs have been successfully prepared and widely used in photovoltaic devices,[3] opto-electronics,[4] and biological analysis.[5]

Inspired by the unique 2D feature of graphene and TMDs, considerable efforts have been devoted to the exploration of new members in the 2D family. As a typical example, black phosphorus (BP), a conceptually new layered material, has triggered a recent resurgence of interest owing to its unique structure as well as fascinating optical and electronic properties.[6] As bulk BP consists of puckered layers stacked together by weak van der Waals interactions, the mechanical exfoliation method has been successfully used to prepare single- and few-layer BP nanosheets.[6a,7] Importantly, BP has a layer-dependent bandgap, which can be tuned from 0.3 to 2 eV as its thickness decreased from bulk to monolayer.[6c,8] The appealing tunable bandgap of BP holds great promise in bridging the space between zero-gap graphene[1a] and large-gap TMDs (1–2 eV).[1f] Moreover, it has been theoretically predicted that the bandgaps of its monolayer (phosphorene) and nanoribbon are highly sensitive to the plane strain and edge structures.[9] Based on its intriguing properties, BP nanosheets have been used in field-effect transistors (FETs),[6a,d] and theoretically predicted for thin film solar-cell[10] and gas sensing[11] applications. Despite the recent progress in mechanically exfoliated BP nanosheets, it is still a challenge to prepare new BP nanostructures in high yield, especially through solution-based approaches.

Herein, for the first time, we report a facile solution-based method for the preparation of black phosphorus quantum dots (BPQDs) from the bulk BP crystal. The as-synthesized BPQDs with average size of 4.9 ± 1.6 nm and thickness of 1.9 ± 0.9 nm (that is, about 4 ± 2 layers) showed good stability in N-monthylpyrrolidinone (NMP). As a proof-of-concept

[*] X. Zhang
Energy Research Institute @ NTU (ERI@N)
Interdisciplinary Graduate School
Nanyang Technological University
50 Nanyang Drive, Singapore 637553 (Singapore)
X. Zhang, Z. D. Liu,[+] C. L. Tan, Dr. Z. M. Luo, Dr. H. Li, Prof. Z. C. Xu, Prof. H. Zhang
School of Materials Science and Engineering
Nanyang Technological University
50 Nanyang Avenue, Singapore 639798 (Singapore)
E-mail: hzhang@ntu.edu.sg
Homepage: http://www.ntu.edu.sg/home/hzhang/
Prof. H. M. Xie,[+] Dr. L. Q. Sun
National & Local United Engineering Lab for Power Battery
Northeast Normal University, Changchun, Jilin 130024 (China)
J. D. Lin, Prof. W. Chen
Department of Physics, National University of Singapore
2 Science Drive 3, Singapore 117542 (Singapore)
Z. D. Liu,[+] Prof. L. H. Xie, Prof. W. Huang
Key Laboratory for Organic Electronics and Information Display & Institute of Advanced Materials (IAM), Jiangsu National Synergistic Innovation Center for Advanced Materials (SICAM), Nanjing University of Posts & Telecommunications
9 Wenyuan Road, Nanjing 210023 (China)
Dr. H. Li, Prof. W. Huang
Key Laboratory of Flexible Electronics (KLOFE) & Institute of Advanced Materials (IAM), Jiangsu National Synergistic Innovation Center for Advanced Materials (SICAM), Nanjing Tech University (NanjingTech)
30 South Puzhu Road, Nanjing 211816 (China)
[+] These authors contributed equally to this work.

[**] This research was supported by MOE under AcRF Tier 2 (ARC 26/13, No. MOE2013-T2-1-034), AcRF Tier 1 (RG 61/12, RGT18/13, and RG5/13), Start-Up Grant (M4080865.070.706022) in Singapore. This research was also conducted as part of the NTU-HUJ-BGU Nanomaterials for Energy and Water Management Program of the Campus for Research Excellence and Technological Enterprise (CREATE), which is supported by the National Research Foundation, Prime Minister's Office, Singapore. H.M.X. thanks a grant support from the National Natural Science Foundation of China (No.21443001). L.H.X. acknowledges the financial support from the National Natural Science Funds for Excellent Young Scholar of China (Grant No. 21322402).

Supporting information for this article is available on the WWW under http://dx.doi.org/10.1002/anie.201409400.

application, the mixture of BPQDs and polyvinylpyrrolidone (PVP), referred to as BPQD-PVP, was used as active layer for the fabrication of flexible memory device, which exhibited a nonvolatile rewritable memory effect with high ON/OFF current ratio of more than 6.0×10^4 and good stability.

Bulk BP crystal, the most stable allotrope of phosphorus, is composed of layered orthorhombic crystal structure with the space group *Cmca* (no. 64), in which the van der Waals interaction is along the crystal *y* axis (Figure 1 a). In each BP layer, which is composed of a puckered honeycomb structure, each P atom bonds with three others, of which three of these atoms are located at the same plane while the forth is in the parallel adjacent plane (Figure 1 b,c).

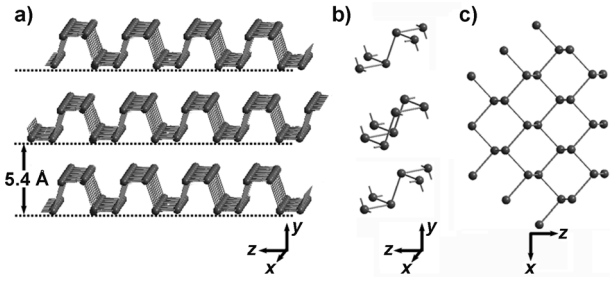

Figure 1. Layered crystal structure of bulk black phosphorus (BP). a) Schematic diagram of BP crystal. b) Three adjacent puckered sheets with linked phosphorus atoms. c) Top view of (a).

The micrometer-sized bulk BP crystals were synthesized from red phosphorus under high pressure and high temperature.[12] The detailed characterization of bulk BP is illustrated in the Supporting Information, Figures S1 and S2. Despite varying the size and shape with no obvious lamellar features (Supporting Information, Figure S2a), the crystalline BP flakes can be obtained after 10 min sonication of bulk BP in NMP (Supporting Information, Figure S2b,c,d). The liquid exfoliation method is commonly used to isolate 2D layered materials and prepare QDs.[1c,13] However, graphene and MoS_2 QDs prepared by this technique usually suffer from the wide size distribution and quite low yield. Bearing this in mind, we combined grinding and sonication processes to exfoliate bulk BP crystals and high-yield BPQDs were obtained.

The morphology of as-prepared BPQDs was characterized by transmission electron microscopy (TEM) and atomic force microscopy (AFM). From TEM images in Figure 2 a,b, the average size of BPQDs is 4.9 ± 1.6 nm (Figure 2 e). High-resolution TEM (HRTEM) images of BPQDs give lattice fringes of 0.34 nm (Figure 2 c) and 0.52 nm (Figure 2 d), which can be ascribed to the (021) and (020) planes of BP crystal, respectively. The AFM image shows the topographic morphology of BPQDs (Figure 2 f). The measured heights of 2.7 and 1.6 nm (Figure 2 g,h) correspond to BPQDs with about 5 and 3 layers, respectively. Statistical AFM analysis gives an average thickness of 1.9 ± 0.9 nm (Figure 2 i), that is, the number of layers being about 4 ± 2 (see the morphology sketch of a BPQD in inset of Figure 2 a).

X-ray photoelectron spectroscopy (XPS) was used to analyze the chemical composition of BPQDs. As seen in the Supporting Information, Figure S3a, the XPS survey shows a predominant P 2p peak at around 129.9 eV and O 1s peak at 532.1 eV. It has been reported that BP is sensitive to water and oxygen and can be degraded to P_xO_y under visible light irradiation.[14] Therefore, the O signal should arise from the oxidation of BP, owing to the exposure of BP sample to the atmosphere before XPS measurement. The high-resolution P 2p spectrum shows two peaks at around 130.3 eV and 129.5 eV (Supporting Information, Figure S3b), assignable to $2p_{1/2}$ and $2p_{3/2}$ binding energy, respectively.[14,15] A peak at high energy region (around 133.9 eV) is indicative of the oxidation of BPQDs (Supporting Information, Figure S3b).

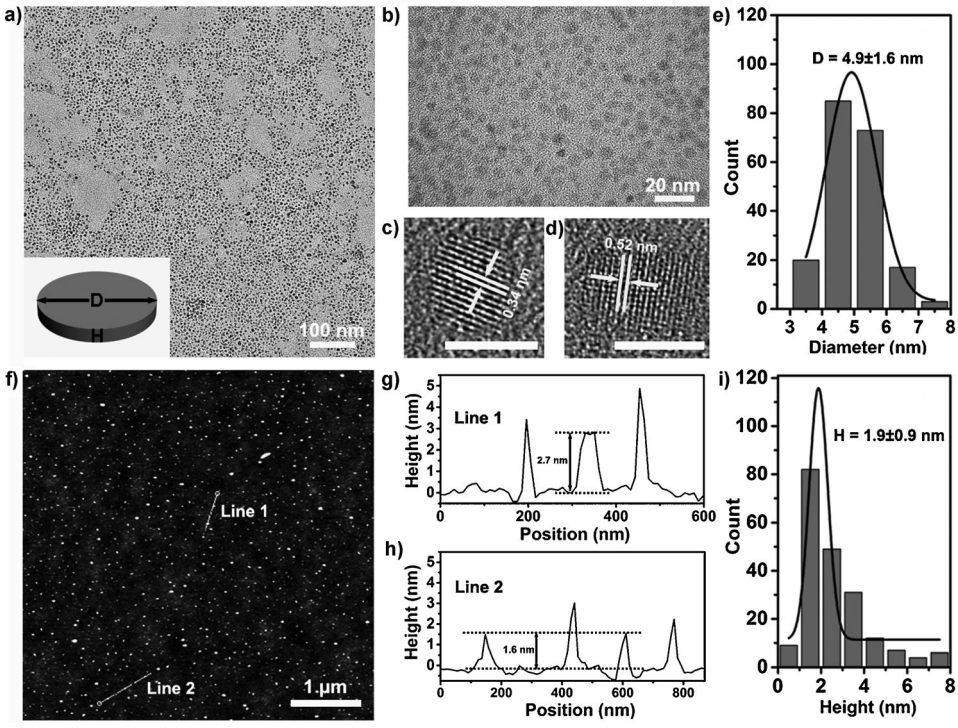

Figure 2. Morphology characterization of BPQDs. a) TEM image of BPQDs. b) Enlarged TEM image of BPQDs. c,d) HRTEM images of BPQDs with different lattice fringes. Scale bar = 5 nm. e) Statistical analysis of the sizes of 200 BPQDs measured from TEM images. f) AFM image of BPQDs. g,h) Height profiles along the white lines in (f). i) Statistical analysis of the heights of 200 BPQDs measured by AFM. A morphology sketch of BPQD is shown as an inset in (a).

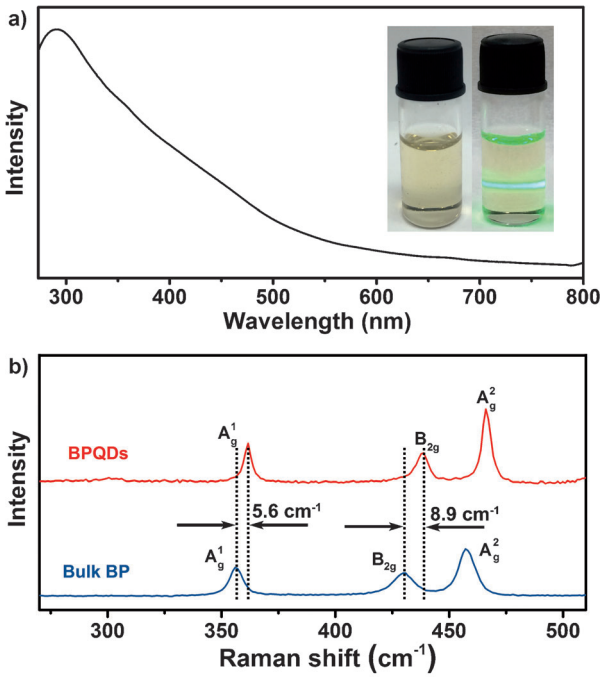

Figure 3. Optical and Raman characterizations of BPQDs. a) UV/Vis absorption spectrum of BPQDs in NMP. Inset: Photos of the BPQD suspension (left) and Tyndall effect of the BPQD suspension (right). b) Raman spectra of BPQDs and bulk crystalline BP.

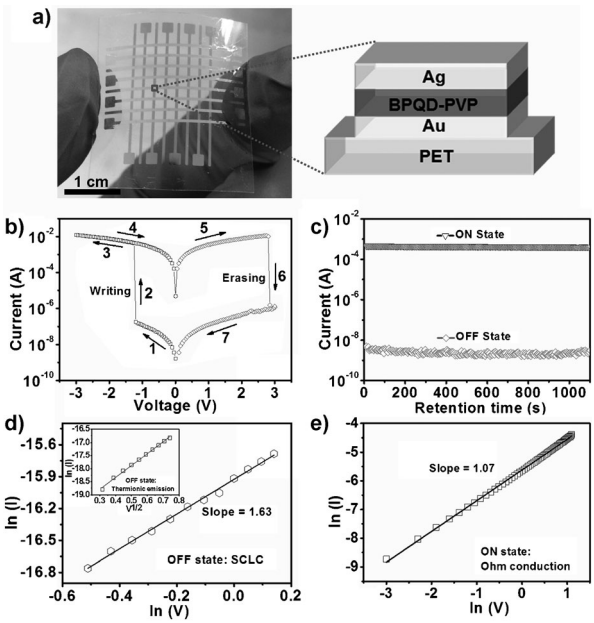

Figure 4. Representation and characterization of the BPQD-based memory device. a) Photograph and illustration of the fabricated flexible memory device. b) The *I*–*V* characteristics of BPQD-based flexible memory device. c) The retention-ability test of BPQD-based memory device in the ON and OFF states at reading voltage of 0.2 V. Experimental data and fitted lines of the *I*–*V* characteristics in the OFF state (d) and ON state (e).

UV/Vis absorption spectroscopy was used to investigate the optical property of BPQDs (Figure 3a). Furthermore, Raman spectroscopy was used to characterize the BPQDs (Figure 3b). Three prominent peaks can be ascribed to one out-of-plane phonon modes (A^1_g) at 361.6 cm^{-1}, and two in-plane modes, that is, B_{2g} and A^2_g, at 438.7 and 466.1 cm^{-1}, respectively. Compared to the bulk BP, both of the B_{2g} and A^2_g modes of BPQDs are blue-shifted by around 8.9 cm^{-1}, while the A^1_g mode is only blue-shifted by 5.6 cm^{-1} (Figure 3b). The frequency difference between A^1_g and B_{2g} modes changes from 73.8 cm^{-1} for bulk BP to 77.1 cm^{-1} for BPQDs. This blue-shift phenomenon is quite similar to the mode change of boron nitride QDs[16] and MoS_2 QDs[17] with thin thickness and small lateral dimensions. The obtained BPQDs can be dispersed in NMP, showing a faint claybank phase (left insert in Figure 3a), which can stabilize without any noticeable aggregation at room temperature for more than 1 month, confirmed by the Tyndall effect (right insert in Figure 3a).

Previous studies have demonstrated that polymer/organic–inorganic hybrid nanomaterials showed a unique conductance-switching effect, and thus can be used in data storage devices.[18] As a proof-of-concept application, after PVP was used as a polymer matrix to mix with BPQDs, referred to as BPQD-PVP, it was used as active layer for memory device with the structure of poly(ethylene terephthalate) (PET)/Au/BPQD-PVP/Ag (Figure 4a). The electronic properties and switching effects were then investigated. As shown in Figure 4b, the BPQD-PVP based device exhibits electrically bistable behavior. Starting with the high-resistance state (HRS) (OFF state) in the device (Stage 1), when the applied negative voltage increased to −1.2 V, the current state increased abruptly from 2.0×10^{-7} to 3.8×10^{-3} A (Stage 2), indicating the electrical property transformed from HRS to low-resistance state (LRS, that is, ON state). The low operating voltage (−1.2 V) is desirable for low-power memory devices. The transition from HRS to LRS is equivalent to a writing process in digital memory devices. This diode shows good stability in the LRS during the subsequent voltage sweep (Stage 3) and can be retained even the power is turned off (Stage 4). It also exhibits good stability in the LRS during the subsequent positive sweep (Stage 5), indicating a nonvolatile effect of the memory. Impressively, the HRS can be recovered by applying a reverse voltage at 2.8 V (Stage 6), which is equivalent to the erasing process of a digital memory device. The device remained in its HRS during the subsequent positive sweep (Stage 7). During the cycle (Stages 1–7), LRS can be maintained even without voltage, but a suitable positive voltage can switch the LRS to HRS. This feature allows the application of BPQD-PVP nanocomposite as the electrically bistable material for flash memory devices.[19] A high ON/OFF current ratio of more than 6.0×10^4 is obtained at the reading voltage of 0.2 V, which is significantly higher than that of C_{60}-PVP,[20] MoS_2-PVP,[21] Au nanoparticle/ZnO nanorod-PVP based diodes.[22] This feature promises a low misreading rate during the device operation. As no switching phenomenon was observed in the pure PVP-based device,[20] BPQDs exhibit an important role in the electrically bistable behavior. To explore the stability of our device, a retention-time test was carried out in the ON and OFF states, which did not undergo obvious fluctuation after a 1.1×10^3 s test under ambient conditions at a reading voltage of 0.2 V (Figure 4c), indicating its good stability.

To understand the carrier transport mechanism of the device, the experimental and fitted data of *I–V* curves are investigated (Figure 4d,e). In the OFF state, the plot of ln(*I*) vs. $V^{1/2}$ from 0 to −0.5 V is fitted to a straight linear (inset in Figure 4d). Such a linear characteristic indicates that the conduction mechanism probably comes from the thermionic emission,[21] arising from the low injection efficiency because of the large barrier between the electrodes and BPQD-PVP active layer.[23] During this process, the charge injection from electrode to the active layer is dominant. After that, a linear relation was observed in the plot of ln(*I*) vs. ln(*V*) for the voltage sweep from −0.5 V to −1.2 V with a slope of 1.63, suggesting that space–charge-limited current (SCLC) dominates the carrier transport process.[21] During this process, charges were transferred from PVP to BPQDs, and then trapped by BPQDs, owing to the lower energy level of BPQDs compared to PVP[23] and a lower free carrier density than the trap density induced by BPQDs, following the SCLC model. With the further increase of bias to exceed the switching voltage, the injected carriers increase exponentially, resulting in the abrupt current transition. After this transition, almost all of the traps are occupied by charges. Consequently, the device shows the ohmic behavior in the ON state (Figure 4e). Moreover, owing to the insulating property of the PVP dielectric material used as matrix, the trapped charges in BPQDs are retained after the power off, which enables the high conductivity and nonvolatility of the memory device. When a reverse voltage is applied, the trapped charges will be detrapped. The internal electrical field induced by the trapped charges disappears. Therefore, the device returns to its initial HRS, and the erasing process of data storage is performed.

In conclusion, for the first time we have successfully synthesized BPQDs from its bulk crystal by a facile solution-based method. The as-prepared BPQDs have lateral size of 4.9 ± 1.6 nm and thickness of 1.9 ± 0.9 nm (ca. 4 ± 2 layers). As a proof-of-concept application, the memory performance of BPQD-PVP was investigated, which showed a flash memory effect with a high ON/OFF current ratio of more than 6.0×10^4 with good stability. It is believed that the new BPQDs might open up more applications in electronics, solar cells, sensing and bio-imaging.

Experimental Section

N-methyl-2-pyrrolidone (NMP, 99.5%, anhydrous), polyvinylpyrrolidone (PVP, MW = 130000), and dichloromethane (≥99.8%, anhydrous) were purchased from Sigma Aldrich. Tetrahydrofuran (THF, analytic reagent grade) was purchased from Fisher Scientific. Poly(ethylene terephthalate) (PET, 0.3 mm thick) was obtained from 3M Company (St. Paul, MN, USA). All the materials were used as received without any further purification.

Bulk black phosphorus (BP) was synthesized from red phosphorus at pressure of 4 GPa and temperature of 800 °C for 10 min, which was described in the previous report.[12] The obtained bulk BP was kept in a glove box filled with Ar gas (< 0.1 ppm H_2O and < 0.1 ppm O_2) prior to use. In a typical experiment for the synthesis of BPQDs, 5 mg of BP powder was added into 1 mL of NMP in a mortar and then ground for 20 min. The mixture was transferred to a glass vial containing 3 mL of NMP. After it was sealed carefully, the vial was taken out from glove box and sonicated in an ice-bath for 3 h at the power of 200 W. The resultant dispersion was centrifuged for 20 min at speed of 7000 rpm. The supernatant containing BPQDs was decanted gently. Except for the sonication and centrifugation processes, other experiments were conducted in a glove box.

Fabrication of BPQD-based memory devices: After 1 mL of BPQD suspension in NMP was centrifuged at 12000 rpm for 20 min, the supernatant was removed and the precipitate was re-dispersed in 1 mL of THF, which was then dispersed in 1 mL PVP solution in THF (10 mg mL^{-1}) to form the mixture of BPQDs and PVP, referred to as BPQD-PVP. After sonication of the mixture for 10 min, it was spin-coated on a PET substrate, which was patterned with 100 nm Au line electrodes (width = 0.5 mm, length = 25 mm), at 1000 rpm for 10 s and then 3000 rpm for 30 s. After drying in an vacuum oven at 60 °C for 6 h, 100 nm thick Ag line electrodes (width = 0.5 mm, length = 25 mm), perpendicular to the Au bottom line electrodes, were deposited by thermal evaporation under vacuum of 10^{-6} Torr with shadow mask. As a result, 8×8 device arrays with BPQD-PVP as the active layer were prepared. The device structure is referred to as PET/Au/BPQD-PVP/Ag (Figure 4a).

Characterization: The BPQD suspension was dropped onto an ultrathin carbon-coated holey carbon support film with 300 mesh copper grid for TEM measurement, and onto a clean Si substrate for Raman and XPS measurement. TEM images were taken with JEOL-2100F at an acceleration voltage of 200 kV. SEM images were obtained using a field-emission scanning electron microscope (FE-SEM, JEOL JSM-7600F). X-ray diffraction (XRD) measurement was performed on a Shimadzu XRD-600 with Cu Kα radiation (λ = 0.15405 nm). UV/Vis absorption spectra were recorded on a CARY 5000 spectrophotometer (Agilent) with QS-grade quartz cuvettes (111-QS, Hellma Analytics) at room temperature. Raman spectra were measured by using a 532 nm micro-Raman spectrometer (Renishaw INVIA Reflex) with the 1800 lines mm^{-1} grating at room temperature. The Raman band of a silicon wafer at 520 cm^{-1} was used as a reference to calibrate the spectrometer. The *I–V* measurement was performed by using a Keithley 4200 semiconductor parameter analyzer under ambient conditions. X-ray photoelectron spectroscopy (XPS) survey was taken in a home-made ultra-high-vacuum system with Mg Kα (1253.6 eV) as excitation source. AFM (Dimension ICON with NanoScope V controller, Bruker, USA) was used to characterize the BPQDs in tapping mode in air. The AFM sample was prepared as follows: after the BPQD suspension in NMP was centrifuged at 12000 rpm for 20 min, the supernatant was removed and the precipitate was re-dispersed in dichloromethane. This process was repeated two times and then the collected suspension was dropped onto a thermally oxidized Si (300 nm SiO_2) substrate cleaned with piranha solution (H_2SO_4/H_2O_2 = 3:1 *v*/*v*) for AFM measurement.

Received: September 23, 2014
Published online: February 3, 2015

Keywords: black phosphorus · memory devices · quantum dots · two-dimensional materials

[1] a) K. S. Novoselov, A. K. Geim, S. V. Morozov, D. Jiang, M. I. Katsnelson, I. V. Grigorieva, S. V. Dubonos, A. A. Firsov, *Nature* **2005**, *438*, 197–200; b) X. Huang, X. Qi, F. Boey, H. Zhang, *Chem. Soc. Rev.* **2012**, *41*, 666–686; c) V. Nicolosi, M. Chhowalla, M. G. Kanatzidis, M. S. Strano, J. N. Coleman, *Science* **2013**, *340*, 1226419; d) X. Huang, Z. Y. Zeng, H. Zhang, *Chem. Soc. Rev.* **2013**, *42*, 1934–1946; e) M. Chhowalla, H. S. Shin, G. Eda, L. J. Li, K. P. Loh, H. Zhang, *Nat. Chem.* **2013**, *5*, 263–275; f) Q. H. Wang, K. Kalantar-Zadeh, A. Kis, J. N. Coleman, M. S. Strano, *Nat. Nanotechnol.* **2012**, *7*, 699–712.

[2] a) K. a. Ritter, J. W. Lyding, *Nat. Mater.* **2009**, *8*, 235 – 242; b) S. N. Baker, G. a. Baker, *Angew. Chem. Int. Ed.* **2010**, *49*, 6726 – 6744; *Angew. Chem.* **2010**, *122*, 6876 – 6896.
[3] Y. Li, Y. Hu, Y. Zhao, G. Shi, L. Deng, Y. Hou, L. Qu, *Adv. Mater.* **2011**, *23*, 776 – 780.
[4] G. Konstantatos, M. Badioli, L. Gaudreau, J. Osmond, M. Bernechea, F. P. G. de Arquer, F. Gatti, F. H. L. Koppens, *Nat. Nanotechnol.* **2012**, *7*, 363 – 368.
[5] a) Q. Liu, B. D. Guo, Z. Y. Rao, B. H. Zhang, J. R. Gong, *Nano Lett.* **2013**, *13*, 2436 – 2441; b) H. D. Ha, D. J. Han, J. S. Choi, M. Park, T. S. Seo, *Small* **2014**, *10*, 3858 – 3862.
[6] a) L. K. Li, Y. J. Yu, G. J. Ye, Q. Q. Ge, X. D. Ou, H. Wu, D. L. Feng, X. H. Chen, Y. B. Zhang, *Nat. Nanotechnol.* **2014**, *9*, 372 – 377; b) H. O. H. Churchill, P. Jarillo-Herrero, *Nat. Nanotechnol.* **2014**, *9*, 330 – 331; c) F. Xia, H. Wang, Y. Jia, *Nat. Commun.* **2014**, *5*, 4458; d) M. Buscema, D. J. Groenendijk, S. I. Blanter, G. A. Steele, H. S. J. van der Zant, A. Castellanos-Gomez, *Nano Lett.* **2014**, *14*, 3347 – 3352.
[7] H. Liu, A. T. Neal, Z. Zhu, Z. Luo, X. Xu, D. Tománek, P. D. Ye, *ACS Nano* **2014**, *8*, 4033 – 4041.
[8] a) D. Warschauer, *J. Appl. Phys.* **1963**, *34*, 1853 – 1860; b) V. Tran, R. Soklaski, Y. Liang, L. Yang, *Phys. Rev. B* **2014**, *89*, 235319.
[9] a) A. S. Rodin, A. Carvalho, A. H. C. Neto, *Phys. Rev. Lett.* **2014**, *112*, 176801; b) X. Peng, A. Copple, Q. Wei, *J. Appl. Phys.* **2014**, *116*, 144301.
[10] J. Dai, X. C. Zeng, *J. Phys. Chem. Lett.* **2014**, *5*, 1289 – 1293.
[11] L. Kou, T. Frauenheim, C. Chen, *J. Phys. Chem. Lett.* **2014**, *5*, 2675 – 2681.
[12] L. Q. Sun, M. J. Li, K. Sun, S. H. Yu, R. S. Wang, H. M. Xie, *J. Phys. Chem. C* **2012**, *116*, 14772 – 14779.
[13] S. Zhuo, M. Shao, S.-T. Lee, *ACS Nano* **2012**, *6*, 1059 – 1064.
[14] A. Favron, E. Gaufres, F. Fossard, P. L. Levesque, A.-L. Phaneuf-L'Heureux, N. Y.-W. Tang, A. Loiseau, R. Leonelli, S. Francoeur, R. Martel, *ArXiv e-prints* **2014**, *1408*, 0345.
[15] J. F. Moulder, W. F. Stickle, P. E. Sobol, K. D. Bomben in *Handbook of X-ray photoelectron spectroscopy* **1992**, Perkin Elmer, Eden Prairie, MN.
[16] L. Lin, Y. Xu, S. Zhang, I. M. Ross, A. C. M. Ong, D. A. Allwood, *Small* **2014**, *10*, 60 – 65.
[17] V. Stengl, J. Henych, *Nanoscale* **2013**, *5*, 3387 – 3394.
[18] a) J. Ouyang, C.-W. Chu, C. R. Szmanda, L. Ma, Y. Yang, *Nat. Mater.* **2004**, *3*, 918 – 922; b) X.-D. Zhuang, Y. Chen, G. Liu, P.-P. Li, C.-X. Zhu, E.-T. Kang, K.-G. Noeh, B. Zhang, J.-H. Zhu, Y.-X. Li, *Adv. Mater.* **2010**, *22*, 1731 – 1735.
[19] S.-J. Liu, P. Wang, Q. Zhao, H.-Y. Yang, J. Wong, H.-B. Sun, X.-C. Dong, W.-P. Lin, W. Huang, *Adv. Mater.* **2012**, *24*, 2901 – 2905.
[20] S. Paul, A. Kanwal, M. Chhowalla, *Nanotechnology* **2006**, *17*, 145.
[21] J. Liu, Z. Zeng, X. Cao, G. Lu, L.-H. Wang, Q.-L. Fan, W. Huang, H. Zhang, *Small* **2012**, *8*, 3517 – 3522.
[22] C. W. Lin, T. S. Pan, M. C. Chen, Y. J. Yang, Y. Tai, Y. F. Chen, *Appl. Phys. Lett.* **2011**, *99*, 023303.
[23] K. Sun, M. Vasudev, H.-S. Jung, J. Yang, A. Kar, Y. Li, K. Reinhardt, P. Snee, M. A. Stroscio, M. Dutta, *Microelectron. J.* **2009**, *40*, 644 – 649.

